

Structural, electronic and magnetic properties of $\text{La}_{1.5}\text{Ca}_{0.5}(\text{Co}_{0.5}\text{Fe}_{0.5})\text{IrO}_6$ double perovskite

L. Bufaiçal^{a,*}, M. A. V. Heringer^b, J. R. Jesus^b, A. Caytuero^b, C. Macchiutti^b,
E. M. Bittar^b, E. Baggio-Saitovitch^b

^a*Instituto de Física, Universidade Federal de Goiás, 74001-970, Goiânia, GO, Brazil*

^b*Centro Brasileiro de Pesquisas Físicas, Rua Dr. Xavier Sigaud 150, 22290-180, Rio de Janeiro, RJ, Brazil*

Abstract

In this work, we report the synthesis and investigation of structural, electronic, and magnetic properties of $\text{La}_{1.5}\text{Ca}_{0.5}(\text{Co}_{0.5}\text{Fe}_{0.5})\text{IrO}_6$. Our polycrystalline sample forms as a single-phase double perovskite in monoclinic $P2_1/n$ space group. Co and Ir are most likely in bivalent and tetravalent oxidation states, respectively, while Mössbauer spectroscopy indicates that Fe is in a trivalent state. The ac and dc magnetization data suggest a ferrimagnetic behavior resulting from the presence of two antiferromagnetic sublattices at Co/Fe and Ir sites. The large coercive field $H_C \simeq 32$ kOe observed at 10 K, comparable to that of other double perovskites of interest for hard magnets, is discussed in terms of the structural distortion and the spin and orbital magnetic moments of the transition metal ions.

Keywords: Double-perovskite; Ferrimagnetism; Cobalt; Iron; Iridium

1. INTRODUCTION

In the $A_2BB'O_6$ double perovskites (DP), the possibility of accommodation of several distinct elements in both A site with alkaline/rare-earth ions and in B and B' sites with transition metal (TM) ions makes this one of the most extensively investigated structures in the last decades [1]. Different combinations of A and B/B' ions can lead to interesting physical properties such as, for instance, multiferroicity [2], exchange bias [3] and even possibly superconductivity [4].

With respect to magnetic properties, the most interesting phenomena are usually observed for combination of 3d with 4d/5d TM ions at B and B' sites, leading for instance to high temperature (T) ferrimagnetism in $\text{Sr}_2\text{CrOsO}_6$ [5], half-metallic behavior in $\text{Sr}_2\text{FeMoO}_6$ [6] and giant magnetoresistance in $\text{Mn}_2\text{FeReO}_6$ [7]. Despite that, the use of 5d Ir ion in DP compounds have received less attention for many years. But recently, the discussion concerning the

*Corresponding author

Email address: lbufaical@ufg.br (L. Bufaiçal)

existence of excitonic magnetism in the anticipated nonmagnetic $j = 0$ ground state of $5d^4$ Ir^{5+} ions in Sr_2YIrO_6 and Ba_2YIrO_6 have put Ir-based systems in the spotlight [8, 9, 10].

There are, however, some earlier works reporting interesting physical properties due to the extended Ir $5d$ orbitals. For instance, electronic structure calculations have predicted a metallic ground state in $\text{La}_2\text{CoIrO}_6$. But this was not confirmed by experimental results, which showed a FM-like insulating state for this Co- and Ir-based DP [11, 12]. Further studies of this material revealed magnetodielectric effect together with re-entrant spin-glass behavior at low- T [13], whereas Ca^{2+} to La^{3+} partial substitution leads to compensation temperatures and spontaneous exchange bias effect in $\text{La}_{1.5}\text{Ca}_{0.5}\text{CoIrO}_6$ (LCCIO) [14]. For the case of Fe- and Ir-based DPs, the Ca^{2+} to La^{3+} partial substitution in $\text{La}_{2-x}\text{Ca}_x\text{FeIrO}_6$ induces interesting changes in the nature of the microscopic magnetic interactions between the TM ions, where the system evolves from antiferromagnetic (AFM) in the $x = 0$ and 2.0 extremities of the series to FM-like in the $x \sim 1.0$ intermediate region, this being ascribed to changes in Ir formal valence [15].

The delicate balance between the strong spin-orbit coupling (SOC), the Coulomb repulsion, and the crystal field splitting in Ir at octahedral coordination makes the Ir-based DPs very sensitive not only to hole/electron doping at A -site, but also to situations where the chemical doping with ions of same oxidation state acts mainly to change the crystal structure. For example, $\text{Lu}_2\text{NiIrO}_6$ is a ferrimagnetic (FIM) Mott insulator where the Lu smallest ionic radius among the $A_2\text{NiIrO}_6$ ($A = \text{La, Pr, Nd, Sm, Eu, Gd, Lu}$) family leads to the largest structural distortion that in turn enhance the AFM coupling between half-filled $\text{Ni-}e_g$ and partially-filled $\text{Ir-}t_{2g}$ orbitals, resulting in its higher T_C [16].

Doping at the B sites in Ir-based DPs may also lead to interesting results. For instance, very recent density functional theory (DFT) calculation in the aforementioned $\text{Lu}_2\text{NiIrO}_6$ compound has predicted that 50% doping with Cr, Mn or Fe at Ni site results in an electronic transition from Mott-insulating to half-metallic state, in which the admixture of Ir $5d$ orbitals in the spin-majority channel are mainly responsible for the conductivity, while the spin minority channel remains an insulator [17].

In this work, we investigate the combined effect of doping at both A - and B -sites in an Ir-based DP. The structural, electronic and magnetic properties of $\text{La}_{1.5}\text{Ca}_{0.5}(\text{Co}_{0.5}\text{Fe}_{0.5})\text{IrO}_6$ (LCCFIO) polycrystalline sample were studied by means of X-ray powder diffraction (XRD), ac and dc magnetization measurements and Mössbauer spectroscopy. Our results show that LCCFIO forms as a single-phase DP in monoclinic $P2_1/n$ space group. Mössbauer spectroscopy indicates that Fe is in the trivalent state, while magnetization as a function of T and applied field (H) curves suggest mixed-valence for Co and Ir. The magnetometry also revealed an FM-like weak magnetization below 112 K, possibly an FIM behavior, which is mainly discussed in terms of a noncollinear magnetic (NCM) structure where Co/Fe and Ir form two AFM sublattices. The large coercive field $H_C \simeq 32$ kOe observed at low- T is discussed in terms of the

structural distortion and of the valence states of TM-ions.

2. EXPERIMENT DETAILS

A polycrystalline sample of LCCFIO was synthesized by the conventional solid-state reaction method. Stoichiometric amounts of La_2O_3 , CaO , Co_3O_4 , Fe_2O_3 and metallic Ir in powder form were mixed and heated at 800°C for 12 hours in air atmosphere. Later the powder was mixed before a second step at 1200°C for 24 hours. Finally, the material was ground, pressed into a pellet, and heated at 1200°C for additional 24 hours. After this procedure, a dark-black material was obtained in the form of a 10 mm diameter disk.

High-resolution XRD data were collected at room T with Cu K_α radiation operating at 40 kV and 40 mA. The XRD data was carried over the angular range $10 \leq \theta \leq 100^\circ$, with a 2θ step size of 0.01° . Rietveld refinement was performed with GSAS software, and its graphical interface program [18]. ^{57}Fe -Mössbauer measurement was performed in transmission geometry at room T , with a ^{57}Co :Rh source moving in a sinusoidal motion. Experimental data were fitted with the Normos program. The magnetization (M) as a function of T [$M(T)$] and M as a function of H [$M(H)$] measurements were carried out in both zero field cooled (ZFC) and field cooled (FC) modes using a Quantum Design PPMS-VSM magnetometer. The heat capacity data, as well as the ac M as a function of T curves, were also carried in the PPMS, these last being performed in the ZFC mode using the VSM head.

3. RESULTS AND DISCUSSION

The room- T XRD pattern of LCCFIO is shown in Fig. 1. As expected, it is a single-phase DP belonging to monoclinic $P2_1/n$ space group, since both $\text{La}_{2-x}\text{Ca}_x\text{CoIrO}_6$ and $\text{La}_{2-x}\text{Ca}_x\text{FeIrO}_6$ series form in this same space group [15, 20]. The Rietveld refinement indicates $\sim 10\%$ of antisite disorder (ASD) at Co/Fe and Ir sites. The similar scattering factors for Co and Fe in Cu K_α radiation prevent precise information concerning these ions' individual contributions to the ASD. The main parameters obtained from the refinement are displayed in Table 1.

The lattice parameters here observed are fairly close to those reported for LCCIO, for which a detailed investigation of the oxidation states by means of X-ray absorption spectroscopy (XAS), X-ray magnetic circular dichroism (XMCD) and Raman spectroscopy revealed mixed valence for Co, with $\sim 70\%$ and 30% of Co^{2+} and Co^{3+} , respectively [12]. In case of the LCCFIO sample here investigated, Mössbauer indicated trivalent state for Fe, while Co and Ir are more likely in bivalent and tetravalent states, respectively, as will be discussed below. This means that the introduction of Fe^{3+} at Co site leads to a slight decrease of the average B-site ionic radius [19], which may be responsible for the subtle decrease of the unit cell volume (V) of LCCFIO (245.95 \AA^3) in comparison to LCCIO (247.09 \AA^3) [12]. It is established for DP compounds that an increase in

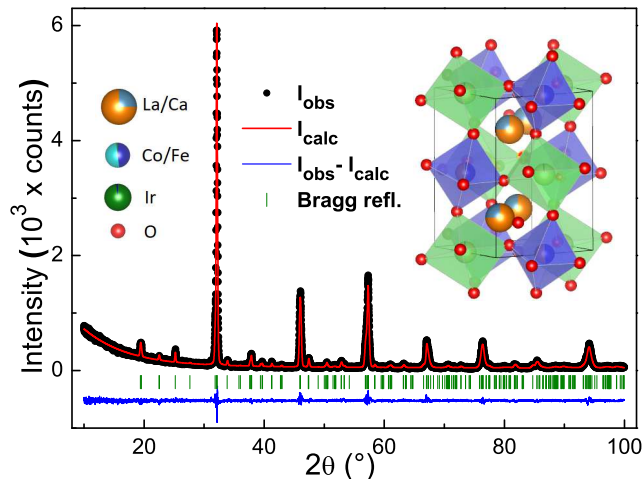


Figure 1: Rietveld refinement fitting of LCCFIO. The vertical lines represent the Bragg reflections for the $P2_1/n$ space group. Inset shows the crystal structure, in which IrO_6 and $(\text{Co/Fe})\text{O}_6$ are drawn as blue and green octahedra, respectively.

the crystal distortion accompanies the volume shrinkage, generally ascribed to tilts in the oxygen octahedra [1], explaining the slightly smaller $(\text{Co/Fe})\text{—O—Ir}$ average bond angle of LCCIO with respect to LCCFIO. Such structural and electronic changes will directly impact the systems’ magnetic properties.

^{57}Fe Mössbauer spectroscopy measurements in transmission geometry were performed on the LCCFIO compound. Fig. 2 shows the Mössbauer spectrum for this perovskite at room T . The model with only one paramagnetic (PM) subspectrum, doublet, showed the best least-squares fit. This analysis indicates that the compound is in its PM state at this temperature and that the Fe ions prefer only one non-equivalent crystallographic site of the structure. From Mössbauer fit, it was also possible to obtain the hyperfine parameters of isomeric shift δ (mm/s), quadrupole splitting ΔE_Q (mm/s), line width Γ (mm/s) and spectral relative area A (%). These parameters are displayed in Table 1, where the isomer shift value is given in relation to $\alpha\text{-Fe}$ [21]. The quadrupole splitting value originates from the electric field gradient formed by the atoms surrounding the Mössbauer probe (^{57}Fe) and may be attributed to an octahedra distortion. A perfect symmetrical octahedron leads to zero quadrupole value. The doublet line width value (~ 0.46) may indicate a structural disorder in this compound. Furthermore, the values of the hyperfine δ and ΔE_Q parameters are consistent with the Fe ions entering the structure with a $3+$ oxidation state [21].

Attempt to perform Mössbauer spectroscopy at low temperature in our LCCFIO sample was not successful. The spectrum (not shown) taken at 3 K, in a Montana cryofree cryostat for 15 days, is poorly resolved displaying high background. This is probably due to the excitation of X-rays of Iridium near to 14.4 keV Mössbauer gamma ray. However, it clearly shows a magnetic sextet with

Table 1: Main parameters obtained from the XRD, Mössbauer, $M(T)$ and $M(H)$ measurements.

a (Å)	b (Å)	c (Å)	β (°)	V (Å ³)
5.5587(1)	5.6178(2)	7.8760(2)	90.0(1)	245.95(2)
$\langle \text{Co/Fe-O-Ir} \rangle$ (°)	ASD (%)	R_{wp}	χ^2	
148.4(1)	9.8(2)	9.7	1.6	
<i>Doublet:</i>		δ (mm/s)	ΔE_Q (mm/s)	Γ (mm/s)
		0.31	0.46	0.46
T_C (K)	T^* (K)	θ_{CW} (K)	μ_{eff} ($\mu_B/\text{f.u.}$)	A (%)
112	85	-118	5.3	100
$M(90\text{kOe})$ ($\mu_B/\text{f.u.}$)	M_s ($\mu_B/\text{f.u.}$)	M_r ($\mu_B/\text{f.u.}$)	H_C (kOe)	
0.56	0.32	0.30	31.7	

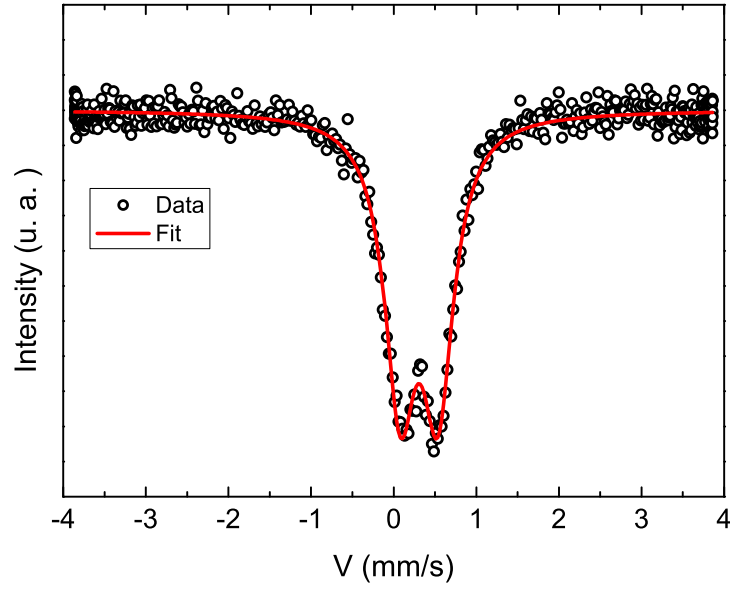


Figure 2: ^{57}Fe Mössbauer spectrum at room temperature showing only one Fe^{3+} site from LCCFIO.

magnetic hyperfine field (Bhf) of 51.4 T and isomer shift (IS) typical of Fe^{3+} , as expected. To make any measurements in the magnetic phase in such kind of material one would probably need to use iron enriched in the ^{57}Fe isotope that has natural abundance of 2.8 %.

Fig. 3(a) displays the ZFC-FC $M(T)$ curves carried at $H = 100$ Oe, showing a FM-like behavior. However, the small low- T magnetization value rules out the possibility of a fully long ranged FM coupling between Fe, Co and Ir. From the fit of the PM region with the Curie-Weiss (CW) law [see inset of Fig. 3(a)], we obtained $\theta_{CW} = -118$ K, fairly close to the magnetic ordering T . The negative sign indicates that AFM coupling is dominant. This, together with the distinct magnetic moments expected for the three different TM ions, suggest FIM behavior.

From the fit with CW law we have also obtained the effective magnetic moment, $\mu_{eff} = 5.3 \mu_B/\text{f.u.}$, which is much larger than the values found for the whole $\text{La}_{2-x}\text{Ca}_x\text{FeIrO}_6$ series ($\sim 4 \mu_B/\text{f.u.}$) [15] and slightly smaller than that found for $\text{La}_{1.5}\text{Ca}_{0.5}\text{CoIrO}_6$ ($5.4 \mu_B/\text{f.u.}$) [12]. For the FeIr-based series, Mössbauer spectroscopy has shown that Fe remains trivalent for all investigated samples [20], as for the LCCFIO sample here investigated. On the other hand, for $\text{La}_{2-x}\text{Ca}_x\text{CoIrO}_6$ a thorough investigation using XAS, XMCD and Raman spectroscopy indicated changes in both Co and Ir oxidation states upon Ca^{2+} to La^{3+} partial substitution [12]. In order to figure out the electronic configurations of Co and Ir in LCCFIO, one can appeal to the following equation commonly used to compute the theoretical magnetic moment of systems consisting of two or more different magnetic ions [20, 22]

$$\mu = \sqrt{\mu_1^2 + \mu_2^2 + \mu_3^2 + \dots} \quad (1)$$

To ensure charge balance, the TM ions must have a total oxidation state of +6.5 in LCCFIO. Since the Mössbauer indicates Fe^{3+} state, we start assuming that Fe^{3+} replaced Co^{2+} in LCCIO, resulting in the $\text{La}_{1.5}\text{Ca}_{0.5}\text{Co}_{0.5}^{3+}\text{Fe}_{0.5}^{3+}(\text{Ir}_{0.5}^{3+}\text{Ir}_{0.5}^{4+})\text{O}_6$ formula. Using the standard magnetic moments for Fe^{3+} ($\mu_{\text{Fe}^{3+}} = 5.9 \mu_B$) and HS Co^{3+} ($\mu_{\text{HS Co}^{3+}} = 5.4 \mu_B$) [23], and assuming for Ir^{4+} the $\mu_{\text{Ir}^{4+}} = 1.7 \mu_B$ value of $J_{1/2}$ state for simplicity ($\mu_{\text{Ir}^{3+}} = 0$), we obtain $\mu = 5.8 \mu_B/\text{f.u.}$ from Eq. 1, rather above the experimental value. Since the delicate balance between the crystal field splitting and the intra-orbital Coulomb repulsion in Co^{3+} at octahedral coordination makes its spin state very sensitive to any perturbation [3, 24], we have also checked the above formula with Co^{3+} in low spin (LS) configuration ($S = 0$), which resulted in $\mu = 4.3 \mu_B/\text{f.u.}$, far below the experimental result. Such discrepancies were expected since Ir^{3+} is rarely observed in octahedral coordination. If we now assume that Fe^{3+} replaces Co^{3+} in LCCIO, the charge neutrality imposes the usual Ir^{4+} configuration, resulting in $\text{La}_{1.5}\text{Ca}_{0.5}\text{Co}_{0.5}^{2+}\text{Fe}_{0.5}^{3+}\text{Ir}^{4+}\text{O}_6$. Using the standard HS Co^{2+} moment ($\mu_{\text{Co}^{2+}} = 4.8 \mu_B$ [23]) we get $\mu = 5.6 \mu_B/\text{f.u.}$, still larger but now closer to the experiment, thus indicating that these are the most likely valence states of the TM ions for LCCFIO. The discrepancy to the experimental result may be related to some overestimation of the Co^{2+} orbital contribution, as well as the naive

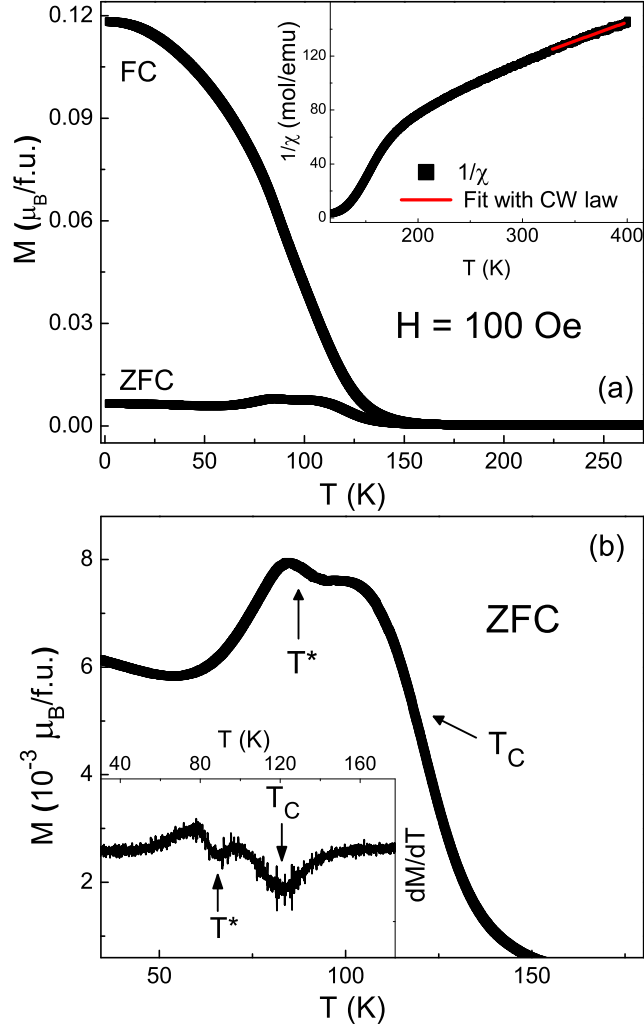


Figure 3: (a) ZFC and FC $M(T)$ curves carried at $H = 100$ Oe. The inset shows the inverse of magnetic susceptibility and the fit of the PM region with the CW law. (b) Magnified view of the ZFC curve around the ordering T . The inset shows its first derivative.

$\mu_{Ir^{4+}} = 1.7 \mu_B$ assumption for the $Ir^{4+} J_{1/2}$ state. Nevertheless, this is not a unique plausible scenario. A detailed investigation employing XAS, XMCD, and neutron powder diffraction (NPD) is mandatory to determine each ions' valence and magnetic moment unambiguously.

An accurate inspection of the ZFC curve, Fig. 3(b), reveals the presence of two anomalies at $T_C = 112$ K and $T^* = 85$ K, and distinct scenarios can be drawn to explain it. The second anomaly could be related to another magnetic transition apart from T_C , in resemblance to the behavior found for other Co- and Fe-based DPs containing three or more magnetic ions [25, 26, 27]. In our case, for instance, the anomalies could be associated respectively to $Co^{2+}-O-Ir^{4+}$ and $Fe^{3+}-O-Ir^{4+}$ couplings, both predicted by the Goodenough-Kanamori-Anderson rules to be of AFM type. On the other hand, they could be related to the distinct magnetic orderings of roughly independent Co/Fe and Ir AFM sublattices, as recently suggested by DFT calculation in La_2CoIrO_6 [28] and corroborated by XMCD and magnetization results in $La_{2-x}Ca_xCoIrO_6$ [12]. Another very plausible scenario is the one in which there is only one magnetic transition and the second anomaly would be related to a crossover, *i.e.* some spin reorientation or structural change not necessarily associated with an order parameter.

To unravel this issue, we performed specific heat (C_p) measurement as a function of temperature, Fig. 4(a). Interestingly, there is no clear transition in the unaided eye C_p curve depicted in the main panel of the figure. However, a magnified view of the C_p/T curve, shown at the inset, indicates a very subtle and broad hump only around T_C , suggestive of a disordered system for which competing magnetic interactions and frustration lead to short-range correlations, in a way that the magnonic contribution is masked by the phononic one which becomes relevant at higher temperatures. Similar behavior is commonly observed in disordered DPs [29, 30, 31]. The absence of anomaly at T^* indicates that this is not related to any conventional magnetic or structural transition. This is in agreement with previous studies of Ir-based DPs as $La_{2-x}Sr_xCoIrO_6$ [11, 32] and La_2ZnIrO_6 [33], for which NPD indicate only one magnetic ordering resulting in NCM with two interpenetrating AFM superstructures for Co/Fe and Ir sites, the weak magnetization observed in these compounds coming from spin canting.

In order to get further insight into the magnetic ordering of LCCFIO, we measured ac M as a function of T with a driving field of 10 Oe and five frequencies (f) in the range 100-10000 Hz. Fig. 4(b) shows the real (χ') and imaginary (χ'') parts of the ac magnetic susceptibility curves, where a peak associated to T_C is clearly observed but at T^* there is again only a subtle kink in χ' , which is unnoticed in the χ'' curves. This agrees with the C_p results, further indicating that this anomaly observed in the magnetization data is not related to a second magnetic ordering. However, one can not completely exclude such possibility since its proximity with the broad and intense peak associated with T_C may be preventing the observation of a subtle second transition in the ac susceptibility and C_p curves. It can also be noticed in the ac magnetization measurements that the magnitude of the peaks change with f for both χ' and χ'' curves. How-

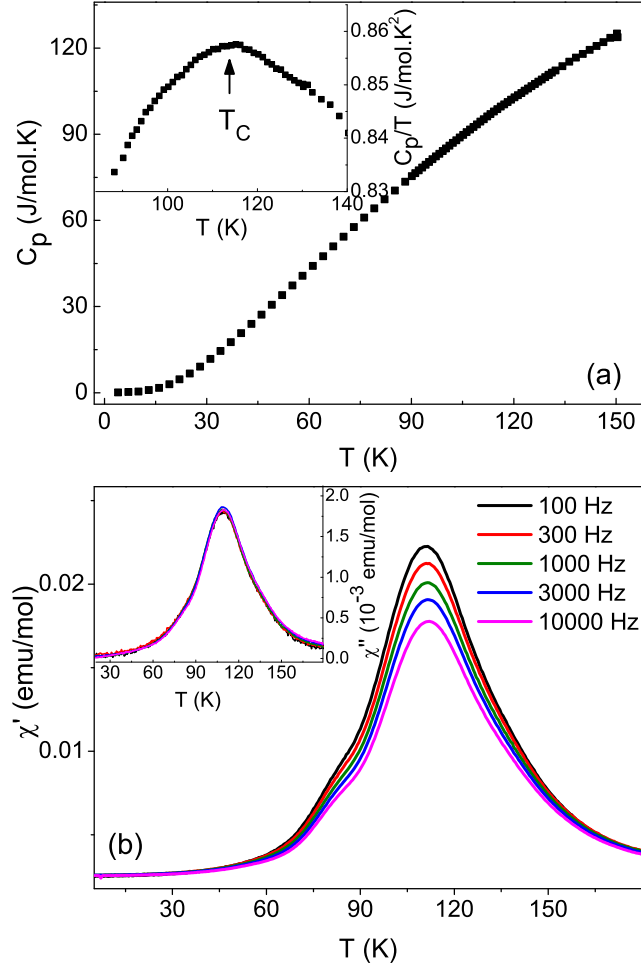


Figure 4: (a) Specific heat (C_p) as a function of T . Inset shows a magnified view of C_p/T near T_C . (b) Real part of the ac magnetic susceptibility (χ') as a function of T , measured with $H_{ac} = 10$ Oe at five different frequencies. Inset shows the imaginary component (χ'').

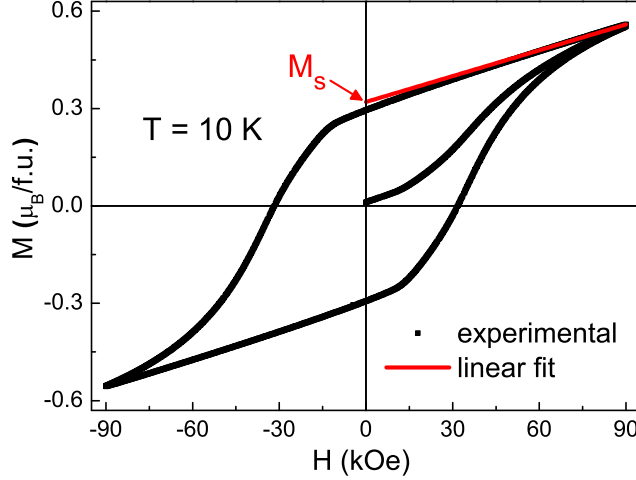


Figure 5: $M(H)$ loop at 10 K. The solid red line is an extrapolated linear fit of the high H data (>80 kOe).

ever, there is no systematic shift of their position in T , ruling out the possibility of some of the peaks being associated with glassy magnetic behavior.

Although the resemblance between LCCFIO and the aforementioned $\text{La}_{2-x}\text{Sr}_x\text{CoIrO}_6$ and $\text{La}_2\text{ZnIrO}_6$ compounds suggests that the most plausible scenario is the one with two AFM sublattices at Co/Fe and Ir sites [11, 32, 33], one must not take precipitate conclusions since a thorough XMCD study of several distinct combinations of Ir and 3d TM ions in DP compounds showed that the magnetic ground state of these Ir-based DPs is susceptible to the structural and electronic environment [34]. Our magnetization data are not enough to unambiguously determine whether the FIM behavior observed in LCCFIO is due to the AFM coupling between the Co/Fe and Ir FM sublattices or NCM from two interpenetration AFM sublattices for Co/Fe and Ir. For this last scenario, the FIM behavior would result from uncompensated Co–Fe AFM coupling or spin canting. Specific measurements such as temperature-dependent XRD, XMCD, and NPD would be necessary to unravel the magnetic structure of LCCFIO.

The $M(H)$ curve can give us further insight into the magnetic ground state of LCCFIO. Fig. 5 displays the hysteresis loop carried out at $T = 10$ K. It is a closed-loop, symmetric with respect to both M and H axes, with an FM-like shape. However, the lack of saturation even at $H = 90$ kOe further indicates AFM coupling between the TM ions, resulting in FIM behavior. The main results extracted from the curve are displayed in Table 1.

The $M_s = 0.32 \mu_B/\text{f.u.}$, obtained from the extrapolation of a linear fit of the high H data (> 80 kOe), as well as the $M = 0.56 \mu_B/\text{f.u.}$ at $H = 90$ kOe (see Table 1), are far below the value expected for a simple linear AFM coupling between two FM sublattices in Ir and Co/Fe sites, even considering the

$\sim 10\%$ of ASD. As aforementioned, NPD studies of $\text{La}_{2-x}\text{Sr}_x\text{CoIrO}_6$ indicated that Co and Ir form two AFM sublattices [11, 32]. Assuming a similar scenario here, *i.e.* an AFM sublattice for Ir and another for Fe/Co, the Ir^{4+} magnetic moments (here considered simply as $J = 1/2$) would cancel. However, the AFM coupling between Fe^{3+} ($S = 5/2$) and Co^{2+} ($S = 3/2$) would not compensate, resulting in FIM behavior. Taking into account that we have 0.5 of Fe^{3+} and 0.5 of Co^{2+} per formula unit, the difference between the moments yields $M = 1.0 \mu_B/\text{f.u.}$, somewhat larger than M_s and $M(90\text{kOe})$. Applying the usual formula to compute the decrease in M due to the ASD [1, 16]

$$M = M_{exp} \times (1 - 2ASD), \quad (2)$$

where M_{exp} is the theoretical SO moment, one has $M = 0.8 \mu_B/\text{f.u.}$, now closer but still larger than the experiment. Such discrepancy to the value expected for a linear Co–Fe AFM coupling gives evidence toward the spin canting scenario, since the small net magnetization values depicted in Table 1 are of the same order of magnitude as those reported for spin canted Ir-based DPs [11, 33]. However, the possibility of NCM with two distinct AFM superlattices for the Fe/Co and Ir sites can not be completely excluded since other ingredients besides ASD may contribute to the further decrease of the magnetization, as for instance antiphase boundaries, oxygen vacancies and defects that could lead to local changes in the TM ions valences, as the afore discussed possible presence of some small amount of Co^{3+} . Again, further investigation is necessary to determine whether the FIM-like behavior of LCCFIO results from uncompensated Co–Fe AFM coupling, from spin canting or even from a simple AFM coupling between Co/Fe and Ir FM sublattices.

Another interesting result obtained from the $M(H)$ curve is the large $H_C \simeq 32 \text{ kOe}$, comparable to those of other DPs of interest for hard magnets [16, 35], and much larger than that reported for LCCIO [12]. Previous studies of chemical pressure on $\text{La}_{1.5}\text{A}_{0.5}\text{CoMnO}_6$ ($A = \text{Ba, Ca, Sr}$) report the increase of H_C with the decrease of the average A -site ionic radius, ascribed to the enhancement of the orbital contribution to the magnetic moments caused by the increased lattice distortion [36]. Conversely, a recent investigation of hydrostatic pressure on A_2FeReO_6 ($A = \text{Ba, Ca}$) has shown a dramatic increase of H_C attributed to pressure-induced changes in the crystal field rather than in the orbital moment [37]. For A_2NiIrO_6 ($A = \text{La-Lu}$), a systematic increase of H_C and T_C was observed with decreasing the unit cell volume, ascribed to the enhanced Ni e_g –Ir t_{2g} orbital hybridization due to lattice distortion [16]. In our case, the great increase in the H_C of LCCFIO with respect to that of LCCIO is certainly not related to the orbital moment of $3d^5 \text{ Fe}^{3+}$ inserted in the system, presumably negligible, but probably to its spin moment and also to the larger structural distortion of the former compound in comparison to the later one, which signifies stronger t_{2g} – t_{2g} orbital hybridization.

4. CONCLUSIONS

In summary, the polycrystalline LCCFIO sample here investigated is a single-phase DP formed in the monoclinic $P2_1/n$ space group with the presence of $\sim 10\%$ of ASD at Co/Fe and Ir sites. Mössbauer spectroscopy analysis revealed that Fe is in a trivalent oxidation state, while the magnetization results indicate mixed-valence for Co and Ir. The magnetization data also revealed a FIM behavior below 112 K, possibly due to the presence of two AFM superstructures for Co/Fe and Ir ions, with the weak net magnetization coming from the uncompensated coupling in the Co/Fe lattice or from spin canting. The significant increase in H_C for LCCFIO with respect to that of LCCIO was discussed in terms of the structural distortions and electronic changes induced by the partial substitution of Co by Fe. Such large H_C is comparable to other DPs of interest for hard magnets, being worth further investigation.

5. ACKNOWLEDGMENTS

This work was supported by Conselho Nacional de Desenvolvimento Científico e Tecnológico (CNPq) [No. 425936/2016-3], Coordenação de Aperfeiçoamento de Pessoal de Nível Superior (CAPES) and Fundação de Amparo à Pesquisa do Estado de Goiás (FAPEG). E.B.S. acknowledges several grants from Fundação Carlos Chagas Filho de Amparo à Pesquisa do Estado do Rio de Janeiro (FAPERJ), including Professor Emeritus fellowship.

References

- [1] S. Vasala and M. Karppinen, Prog. Solid State Chem. 43 (2015) 1.
- [2] M. Azuma, K. Takata, T. Saito, S. Ishiwata, Y. Shimakawa, and M. Takano, J. Am. Chem. Soc. 127 (2005) 24.
- [3] M. Boldrin, A. G. Silva, L. T. Coutrim, J. R. Jesus, C. Macchiutti, E. M. Bittar, and L. Bufaçal, Appl. Phys. Lett. 117 (2020) 212402.
- [4] D. R. Harshman, W. J. Kossler, A. J. Greer, D. R. Noakes, C. E. Stronach, E. Koster, M. K. Wu, F. Z. Chien, J. P. Franck, I. Isaac, and J. D. Dow, Phys. Rev. B 67 (2003) 054509.
- [5] Y. Krockenberger, K. Mogare, M. Reehuis, M. Tovar, M. Jansen, G. Vaitheeswaran, V. Kanchana, F. Bultmark, A. Delin, F. Wilhelm, A. Rogalev, A. Winkler, and L. Alff, Phys. Rev. B 75 (2007) 020404(R).
- [6] K.-I. Kobayashi, T. Kimura, H. Sawada, K. Terakura, and Y. Tokura, Nature 395 (1998) 677.
- [7] M.-R. Li, M. Retuerto, Z. Deng, P. W. Stephens, M. Croft, Q. Huang, H. Wu, X. Deng, G. Kotliar, J. Sánchez-Benítez, J. Hadermann, D. Walker, and M. Greenblatt, Angew. Chem., Int. Ed. 54 (2015) 12069.

- [8] G. Cao, T. F. Qi, L. Li, J. Terzic, S. J. Yuan, L. E. DeLong, G. Murthy, and R. K. Kaul, Phys. Rev. Lett. 112 (2014) 056402.
- [9] L. T. Corredor, G. Aslan-Cansever, M. Sturza, K. Manna, A. Maljuk, S. Gass, T. Dey, A. U. B. Wolter, O. Kataeva, A. Zimmermann, M. Geyer, C. G. F. Blum, S. Wurmehl, and B. Büchner, Phys. Rev. B 95 (2017) 064418.
- [10] S. Fuchs, T. Dey, G. Aslan-Cansever, A. Maljuk, S. Wurmehl, B. Büchner, and V. Kataev, Phys. Rev. Lett. 120 (2018) 237204.
- [11] N. Narayanan, D. Mikhailova, A. Senyshyn, D. M. Trots, R. Laskowski, P. Blaha, K. Schwarz, H. Fuess, and H. Ehrenberg, Phys. Rev. B 82 (2010) 024403.
- [12] L. Bufaiçal, E. Sadrollahi, F. J. Litterst, D. Rigitano, E. Granado, L. T. Coutrim, E. B. Araújo, M. B. Fontes, E. Baggio-Saitovitch, and E. M. Bittar, Phys. Rev. B 102 (2020) 024436.
- [13] J. Song, B. Zhao, L. Yin, Y. Qin, J. Zhou, D. Wang, W. Song, and Y. Sun, Dalton Trans 46 (2017) 11691.
- [14] L. T. Coutrim, E. M. Bittar, F. Stavale, F. Garcia, E. Baggio-Saitovitch, M. Abbate, R. J. O. Mossaneck, H. P. Martins, D. Tobia, P. G. Pagliuso, and L. Bufaiçal, Phys. Rev. B 93 (2016) 174406.
- [15] L. Bufaiçal, L. Mendonça Ferreira, R. Lora-Serrano, O. Agüero, I. Torriani, E. Granado, P. G. Pagliuso, A. Caytuero, and E. Baggio-Saitovich, J. Appl. Phys. 103 (2008) 07F716.
- [16] H. L. Feng, Z. Deng, M. Wu, M. Croft, S. H. Lapidus, S. Liu, T. A. Tyson, B. D. Ravel, N. F. Quackenbush, C. E. Frank, C. Jin, M-R. Li, D. Walker, and M. Greenblatt, Inorg. Chem. 58 (2019) 1.
- [17] S. Nazir, Sci. Rep. 11 (2021) 1240.
- [18] A. C. Larson and R. B. Von Dreele, Los Alamos National Laboratory Report No. LAUR 86-748, 2000; B. H. Toby, J. Appl. Crystallogr. **34**, 210 (2001).
- [19] R. D. Shannon, Acta Crystallographica A32 (1976) 751.
- [20] L. T. Coutrim, D. C. Freitas, M. B. Fontes, E. Baggio-Saitovitch, E. M. Bittar, E. Granado, P. G. Pagliuso, and L. Bufaiçal, J. Solid State Chem. 221 (2015) 373.
- [21] Greenwood N. N. and Gibb T. C. Mössbauer Spectroscopy (1971) (London: Chapman and Hall).
- [22] D. Niebieskikwiat, R. D. Sánchez, A. Caneiro, L. Morales, M. Vásquez-Mansilla, F. Rivadulla and L. E. Hueso, Phys. Rev. B 62 (2000) 3340.

- [23] N. W. Ashcroft and N. D. Mermin, *Solid State Physics*, Cengage Learning (1976).
- [24] B. Raveau and Md. Motin Seikh, *Cobalt Oxides: From Crystal Chemistry to Physics* (Wiley-VCH, Weinheim, 2012).
- [25] R. I. Dass and J. B. Goodenough, Phys. Rev. B 67 (2003) 014401.
- [26] H. G. Zhang, L. Xie, X. C. Liu, M. X. Xiong, L. L. Cao and Y. T. Li, Phys. Chem. Chem. Phys. 19 (2017) 25186.
- [27] J. Krishna Murthy, K. D. Chandrasekhar, H. C. Wu, H. D. Yang, J. Y. Lin and A. Venimadhav, J. Phys.: Condens. Matter 28 (2016) 086003.
- [28] S. Ganguly and S. Bhowal, Phys. Rev. B 101 (2020) 085104.
- [29] A. A. Aczel, D. E. Bugaris, L. Li, J.-Q. Yan, C. de la Cruz, H.-C. zur Loye, and S. E. Nagler, Phys. Rev. B 87 (2013) 014435.
- [30] S. Sharma, K. Singh, R. Rawat, N.P. Lalla, J. Alloys Compd. 693 (2017) 188-193.
- [31] L. Bufaiçal, C. Adriano, R. Lora-Serrano, J. G. S. Duque, L. Mendonça-Ferreira, C. Rojas-Ayala, E. Baggio-Saitovitch, E. M. Bittar, and P. G. Pagliuso, J. Solid State Chem. 212 (2014) 23-29.
- [32] S. Lee, M-C. Lee, Y. Ishikawa, P. Miao, S. Torii, C. J. Won, K. D. Lee, N. Hur, D-Y. Cho, and T. Kamiyama, Phys. Rev. B 98 (2018) 104409.
- [33] H. Guo, C. Ritter, Y. Su, A. C. Komarek, and J. S. Gardner, Phys. Rev. B 103 (2021) L060402.
- [34] M. A. Laguna-Marco, P. Kayser, J. A. Alonso, M. J. Martínez-Lope, M. van Veenendaal, Y. Choi, and D. Haskel, Phys. Rev. B 91 (2015) 214433.
- [35] H. L. Feng, M. Reehuis, P. Adler, Z. Hu, M. Nicklas, A. Hoser, S.-C. Weng, C. Felser, and M. Jansen, Phys. Rev. B 97 (2018) 184407 (2000).
- [36] L. T. Coutrim, D. Rigitano, C. Macchiutti, T. J. A. Mori, R. Lora-Serrano, E. Granado, E. Sadrollahi, F. J. Litterst, M. B. Fontes, E. Baggio-Saitovitch, E. M. Bittar, and L. Bufaiçal, Phys. Rev. B 100 (2019) 054428.
- [37] C. A. Escanhoela, G. Fabbris, F. Sun, C. Park, J. Gopalakrishnan, K. Ramesha, E. Granado, N. M. Souza-Neto, M. van Veenendaal, and D. Haskel, Phys. Rev. B **98**, 054402 (2018).